CONF-760622--46

EVOLUTION OF CLADDING ATTACK IN LMFBR TYPE OXIDE FUEL PINS

J. W. Weber
R. L. Gibby
D. C. Hata
E. T. Weber

May 12, 1976

Presented at the American Nuclear Society Meeting
June 13-18, 1976, at Toronto, Canada

HANFORD ENGINEERING DEVELOPMENT LABORATORY
Richland, Washington
operated by
WESTINGHOUSE HANFORD COMPANY
A SUBSIDIARY OF Westinghouse Electric Corporation
for the
UNITED STATES ENERGY RESEARCH AND DEVELOPMENT ADMINISTRATION
UNDER CONTRACT E(45-1)-2170

EVOLUTION OF CLADDING ATTACK IN LMFBR TYPE OXIDE FUEL PINS

J. W. Weber[1], R. L. Gibby[2], D. C. Hata[1], and E. T. Weber[3]

The HEDL P-23 high cladding temperature tests in EBR-II are yielding data on fuel-cladding chemical interaction (FCCI) from highly characterized mixed oxide fuel pins. In addition to wastage allowance correlations, the observations provide information on the characteristics of cladding attack that is, structural and chemical distribution of fuel, cladding and fission products as a function of temperature and burnup.

Additional examination remains to be done before a full assessment of FCCI in these pins can be completed and mechanisms for the cladding reactions proposed. However, it is of value at this time to present the observations of cladding attack and compare then with other data reported. This irradiation test offers the opportunity to study the character and evolution of FCCI in a common set of fuel pins, all having been irradiated together in the same subassembly and having been fabricated from a consistent lot of fuel and cladding materials.

In this paper, we will describe observations of fuel-cladding chemical interaction on 316-20% cold worked stainless steel over the cladding temperature range 400°C to 750°C. Data at three burnup levels (1.2, 2.4, and 5.0 at%) show the changing character of FCCI with continued exposure.

The fuel pins were irradiated in a 37-pin subassembly in flowing sodium at peak linear power ratings up to 400 W/cm (12 kw/ft). Each pin contained a 34.3 cm (13.5 in.) long fuel column of 25 W/oPuO_2 - 75 W/oUO_2 sintered pellets clad with 0.584 cm (0.230 in.) diameter, 0.038 cm (0.015 in.) thick, 20% cold worked 316 stainless steel tubing. Figure 1 lists the fuel pins and their operating conditions. All fuel pins were fabricated with an oxygen to metal ratio of about 1.98, which is greater than the current upper limit for FFTF/CRBRP reference fuel.

1) Engineers with Performance Analysis, Reference Fuels
2) Manager Fuels Research, Fuel and Control Technology
3) Manager Fuel and Control Technology

It has been shown both by calculation and with measurements on irradiated fuel pins that with slightly hypostoichiometric fuel, such as in these P-23A pins, radial redistribution of oxygen occurs early in life. The oxygen migration down the temperature gradient provides an oxygen activity at the cladding surface sufficient to oxidize the chromium in the cladding. However, based on laboratory studies, significant cladding corrosion is not expected until fission products Cs and Te are available to participate in an enhanced oxidation process. The quantities required are small however, with sufficient quantities being generated by approximately 0.4 at% burnup to initiate the reactions. It is as expected then that even at the lowest burnup in the P-23A pins, significant reaction was observed.

The coolant temperatues and thus the cladding temperatures increase from bottom to top along the fuel pins in the EBR-II subassemblies. The FCCI was characterized as a function of temperatures by examining metallographically section removed at several axial locations along the fuel pin.

Cladding attack was classified as one of four characteristic types also noted in other studies, namely: 1) matrix, 2) intergranular, 3) combined matrix and intergranular, and 4) deep-localized attack. Figures 2 and 3 show typical photomicrographs of matrix and intergranular type of attack. The reaction product of the matrix attack, Figure 2, is a mixture of metallic and nonmetallic compounds in the fuel to cladding gap. The attack of the grains is uniform with no strong preference for attack along the grain boundaries. In the intergranular attack, Figure 3, metallic and nonmetallic reaction products is also visible in the fuel to cladding gap and the grains have been chemically attacked as evidenced by the roughened surface. In addition, however, this photograph shows opening of the grain boundaries from the cladding inside surface indicating that attack is occuring along the grain boundaries.

Several photographs were taken of each transverse section and the dominant reaction type, that is, the type that occurred most generally around the cladding, was determined for each cross section, Figure 4. It needs to be emphasized that characteristic indicated is the most prominent type shown in the large numbers of photos examined. Within a transverse section these reactions were not generally uniform in character, depth, or circumferential extent. For example, where the cladding was not in contact with fuel at the ends of large radial startup cracks on the exterior of the fuel, less reaction was observed than where cladding and fuel were in tight contact. Other

phenomena which might cause local variations in attack include the size of the fuel-to-cladding gap, and the location of certain fission product concentrations such as Cs and Te.

The character of the reactions appeared to be strongly a function of temperature, with a burnup dependence of the higher temperatre range. As shown in Figure 4, no attack was observed below 500°C, consistent with most reported data. At temperatures between 500 and 680° matrix attack was predominant at all three burnup levels. At temperatures of 680°C however, the attack changed from primarily intergranular and deep localized to a matrix form of reaction. We want to emphasize this change in character of reaction with burnup in a sweies of photomicrographs of the fuel cladding interface from P-23A fuel pins starting at intermediate burnup.

Figure 5 shows the typical character of reaction at 2.4 at% burnup at temperatures up to 675°C. The reaction is principally matrix type as shown in the optical picture. Electron microprobe results reveal that the metallic reaction product is composed of Fe (Figure 5), and Ni. Cr and Cs appear next the the cladding in a nonmetallic form as shown in Figure 5. Te is occassionally found with the Cs and Cr. Mn and Mo form nonmetallic layers of high concentration, usually between the Cr + Cs layer and the metallic Fe + Ni reaction product layer. At temperature below 675° however, the attack depth is less and the reaction layer thinner.

Above temperatures of 675°C the character changes as shown in Figure 2 from matrix to intergranular. In Figure 6, the intergranular attack is extensive with some areas of attack up to 25 μm deep. Whole grains on the cladding edge are becoming surrounded by intergranular attack and the carbides are beginning to disappear in them and along the grain boundaries. These observations are an extension of the caracter found at the lower burnup in this temperature range. However, the frequency of its occurrence is much greater. Electron microprobe results show that Cr is being depleted at grain boundaries along which carbides have disappeared.

Now we will describe the character of reaction observed at the highest burnup, $\sim$ 5.0 at%. As at the lower burnup, the predominant attack up to approximately 680°C is matrix type. However, in contrast to the intergranular

attack predominant above 680°C at the lower burnup, the character at 5.0 at% has changed to a matrix appearance, as shown in Figure 7. This form of matrix reaction we prefer to call advanced or evolved matrix attack. Evidence of the change in reaction character was noted in some areas on the fuel pin at 2.4 at% burnup in the temperature range above 680°.

Whole grains have been lost or detached from the cladding. In other grains still attached to the cladding, the carbides have completely disappeared. Electron microprobe results, Figures 8 and 9, reveal that the grains and grain boundaries where carbides have disappeared are depleted in Cr, leaving Fe + Ni enhanced areas similar to results at lower burnup but much more extensive. The Cs and Cr are present together in a nonmetallic form, probably an oxide, next to the cladding Figure 10, but they are now very localized in high concentrations adjacent to the chromium depleted grains. Layers of Mn and Mo are found in the gap between the Fe and Ni reaction product and the Cs + Cr layer. There is no fission products down into the grains or grain boundaries where carbides have disappeared.

Thus by using a data base of fuel pins all from one subassembly, that are consistent in fuel cladding and history we have been able to characterize the structure and chemical composition changes occurring in the reaction between fuel, fission product and cladding as a function of temperature and burnup.

From these observations, we can summarize the important points in the evolution of fuel-cladding chemical interaction, as shown in Figure 11.

1. Etched cladding revealed grain boundaries in which carbides have disappeared or, as sometimes labeled, "latent" attack, has occurred ahead of the optically observed attack front.

2. At the two lower burnups of 1.2 and 2.4 at%, there is a consistent division of the types of reaction, with a predominantly matrix attack at temperatures below 680°C and a predominantly intergranular attack at temperatures above 680°C.

3. The type of attack at 680°C changed from intergranular at the intermediate burnup of 2.4 at% to predominantly matrix attack at the highest burnup of 5.3 at%. As the intergranular attack progresses, it tends to surround whole grains, depleting them of Cr and exposing greater surface area to attack.

4. Electron microprobe data revealed that the grains and grain boundaries in which carbides had disappeared were depleted of Cr. A nonmetallic reaction product of Cr, Cs and, occassionally, Te is found in the gap next to the reaction front. No fission product Cs or Te has been detected in the chromium depleted latent attack grain boundaries or grains.

5. Of significance to the loss of cladding and the the ultimate effect on fuel pin performance are those changes in character of cladding attack that occur at temperatures greater than 675°C as the burnup increases above 2.4 at%. This change in type of attack from a predominantly intergranular form to a matrix, presents greater surface area of the cladding upon which reaction can occur. This may account for the observed slowing of the rate at which the depth of attack increases with burnup.

FUEL PINS EXAMINED FOR FUEL CLADDING CHEMICAL INTERACTION

PIN	FUEL O/M	PEAK FUEL BURNUP AT. %	PEAK LINEAR POWER W/cm	EXPOSURE TIME DAYS	MAXIMUM CLADDING TEMPERATURE °C
P-23A					
58B	1.98	1.2	387	46	708
59C	1.98	1.2	386	46	709
60D	1.98	1.3	404	48	723
62F	1.98	1.3	402	48	749
26	1.98	2.3	394	94	743
31	1.98	2.3	393	94	726
63G	1.98	2.5	378	98	729
25	1.98	5.0	366	192	725

HEDL 7605-140.13

FIGURE 1

FUEL CLADDING INTERFACE

T_{CLAD} SURFACE - 575°C TO 675°C
FUEL BURNUP - 1.2 AT. %
MATRIX REACTION

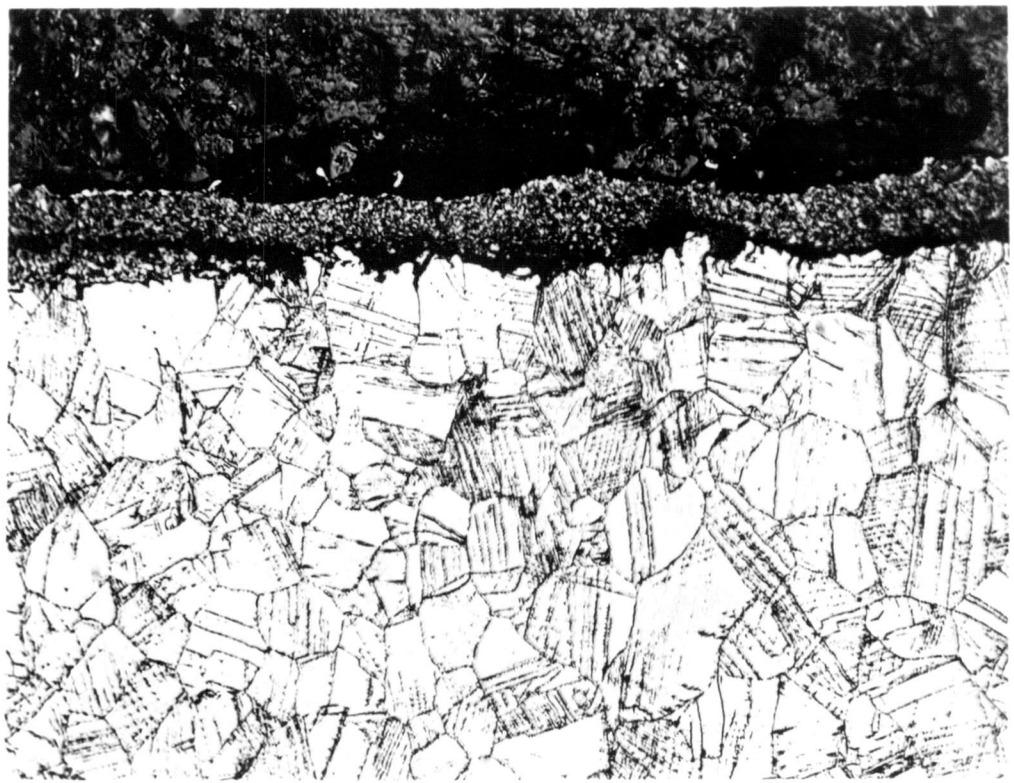

20 μm

HEDL 7605-140.16
FIGURE 2

FUEL CLADDING INTERFACE

$T_{CLAD\ SURFACE}$ - 690°C

FUEL BURNUP - 1.2 AT. %

O/M - 1.98

INTERGRANULAR REACTION

20 μm

HEDL 7605-140.17

FIGURE 3

DOMINANT CHARACTER OF FUEL CLADDING CHEMICAL INTERACTION

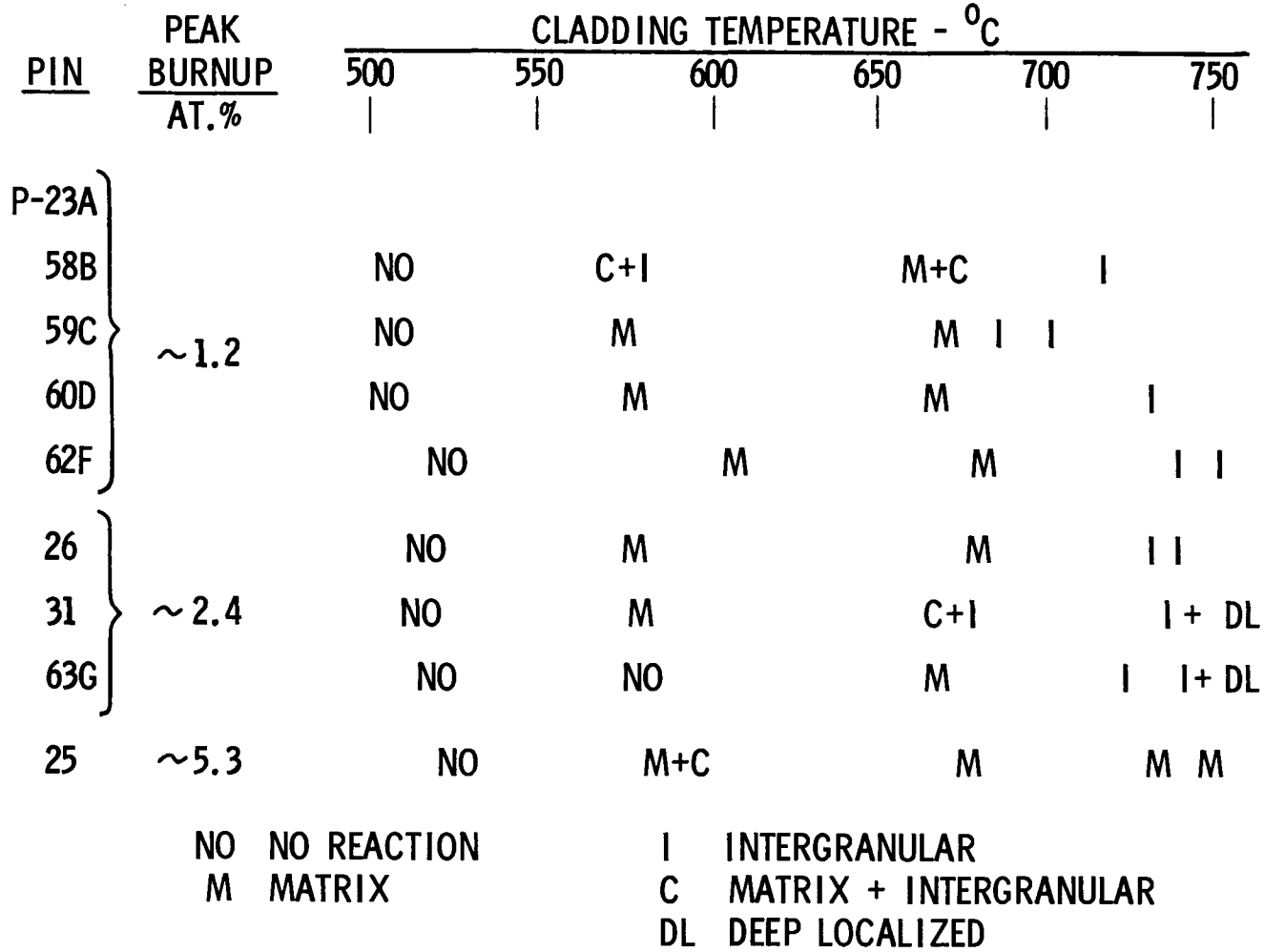

HEDL 7605-140.11

FIGURE 4

CLADDING AND FISSION PRODUCT DISTRIBUTION IN MATRIX REACTION

T_{CLAD} SURFACE - 671°C

FUEL BURNUP - 2.4 AT. %

O/M - 1.98

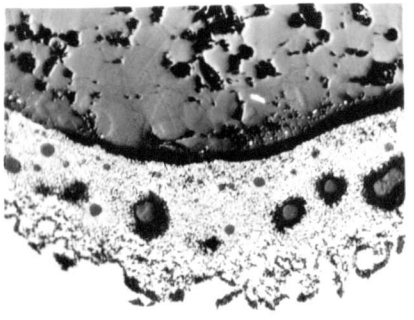

OPTICAL

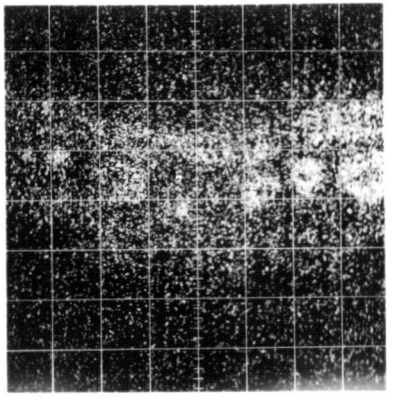

CESIUM NEG 311-18

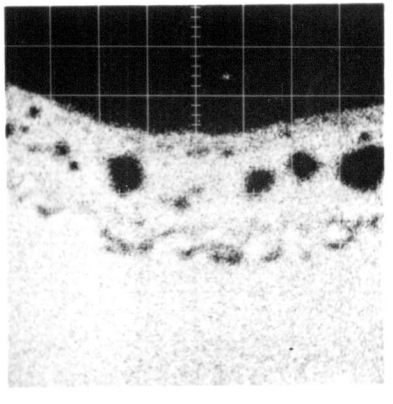

IRON NEG 311-13

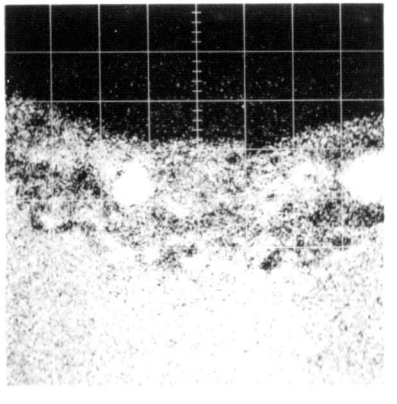

CHROMIUM NEG 311-14

HEDL 7605-140.18

FIGURE 5

FUEL CLADDING INTERFACE

T_{CLAD} SURFACE - $>675^{o}C$

FUEL BURNUP - 2.4 AT. %

O/M 1.98

INTERGRANULAR REACTION

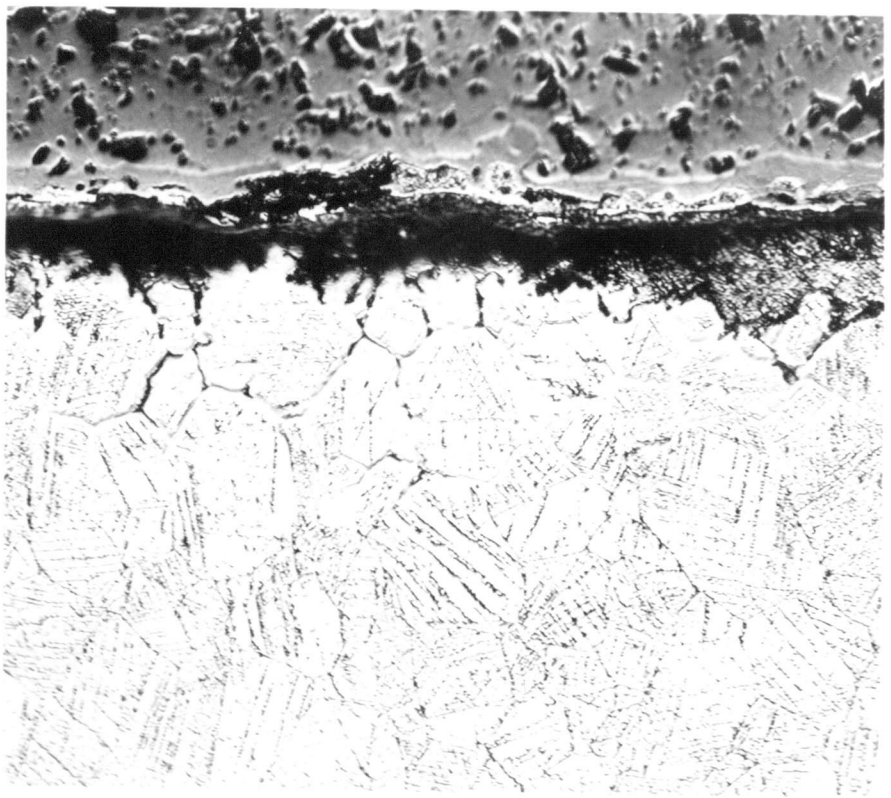

20 μm

HEDL 7605-140.19

FIGURE 6

FUEL CLADDING INTERFACE

T_{CLAD} SURFACE - $>680^{o}C$

FUEL BURNUP - 5.3 AT. %

O/M - 1.98

ADVANCED MATRIX REACTION

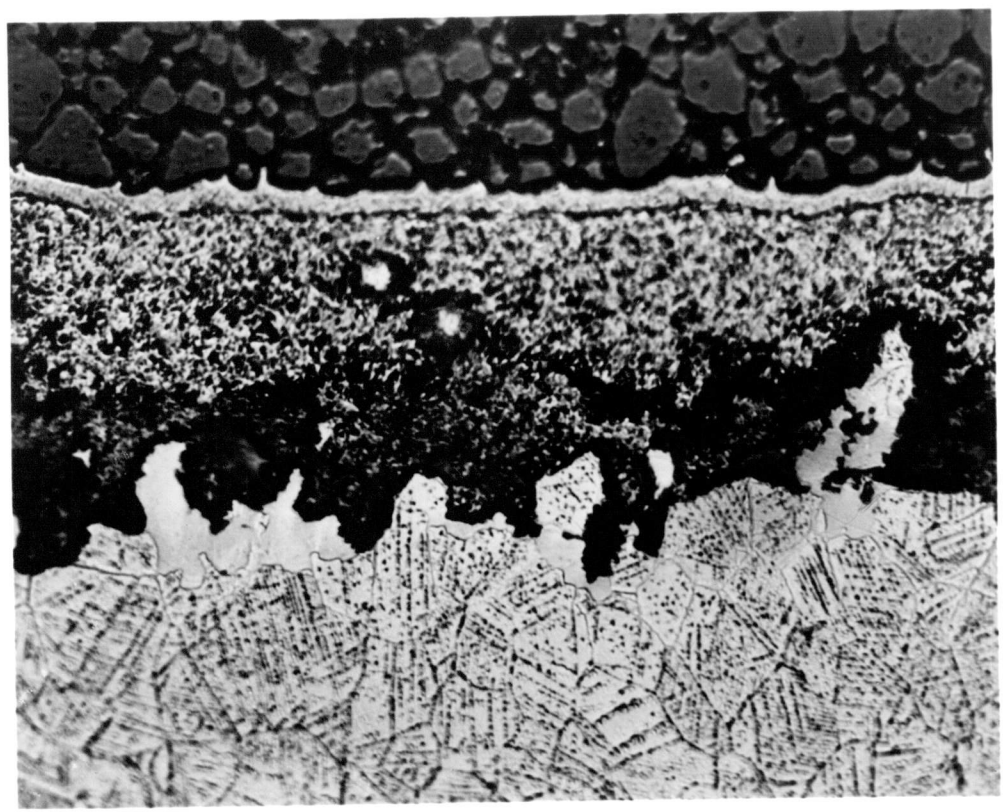

20 μm

HEDL 7605-140.20

FIGURE 7

CLADDING AND FISSION PRODUCT DISTRIBUTION IN ADVANCED MATRIX REACTION

T_{CLAD} SURFACE - > 680°C
FUEL BURNUP - 5.3 AT. %

O/M - 1.98

20 μm

20 μm

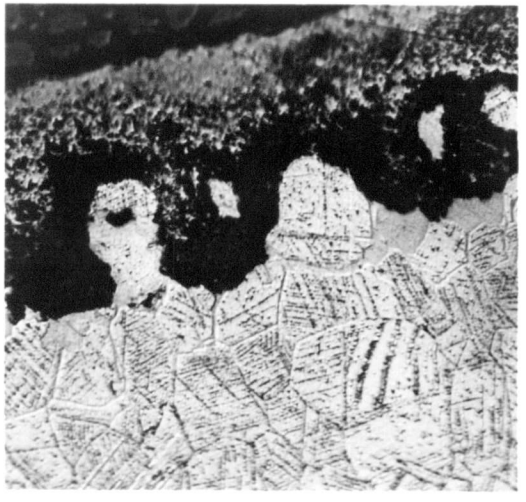

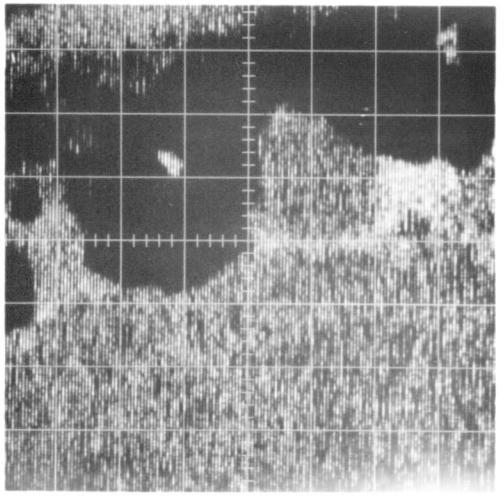

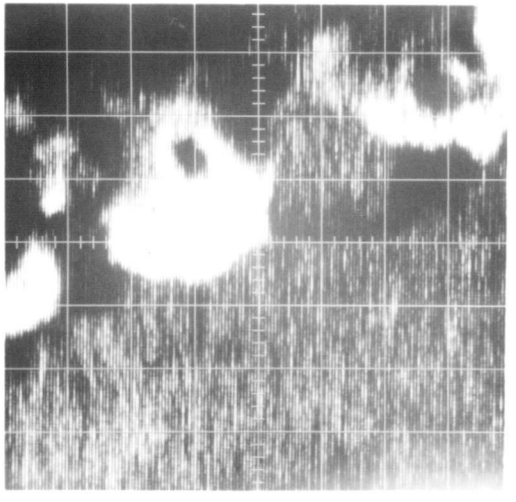

OPTICAL

IRON

CHROMIUM

HEDL 7605-140.24

FIGURE 8

DISTRIBUTION OF CLADDING ELEMENTS IN ADVANCED MATRIX REACTION

T_{CLAD} SURFACE - 660°C
FUEL BURNUP - 5.3 AT. %

O/M - 1.98

20 μm

20 μm

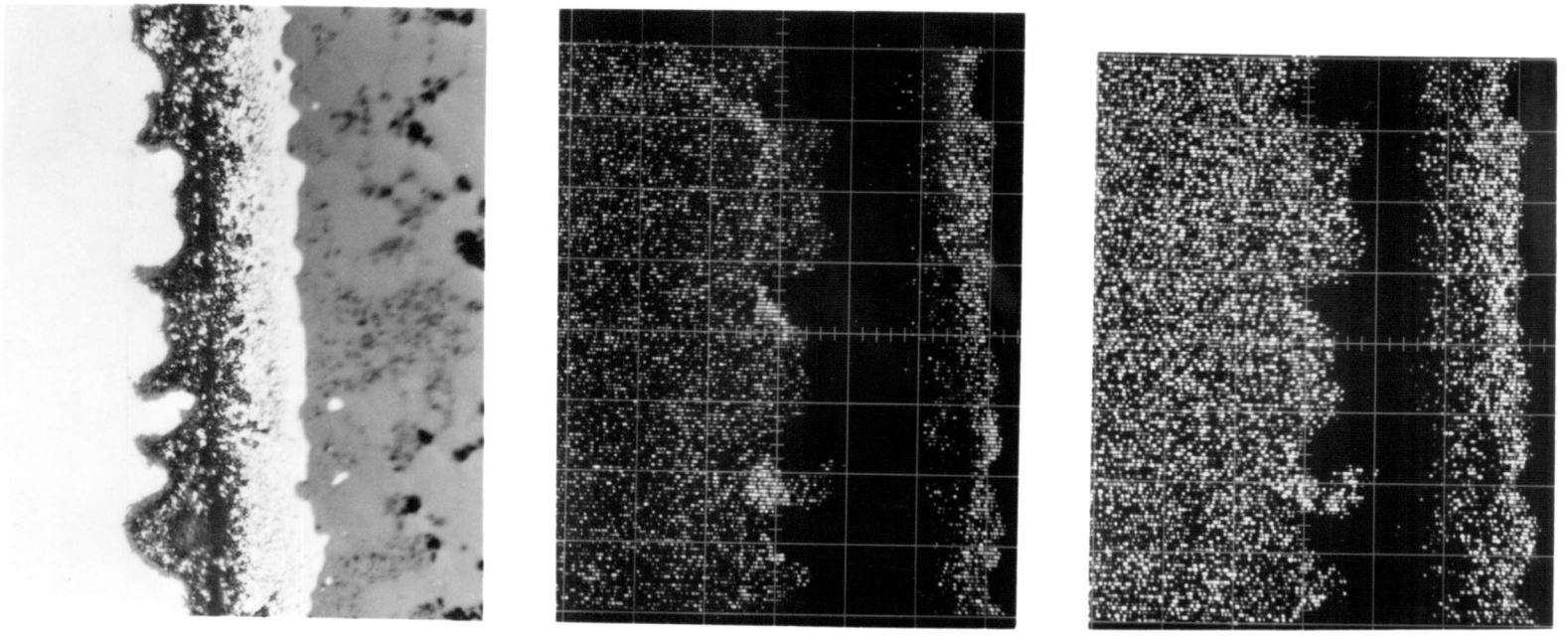

CLADDING FUEL IRON NICKEL

HEDL 7605-140.23

FIGURE 9

DISTRIBUTION OF CHROMIUM AND CESIUM IN ADVANCED MATRIX REACTION

T_{CLAD} SURFACE - 660°C
FUEL BURNUP - 5.3 AT. %

O/M - 1.98

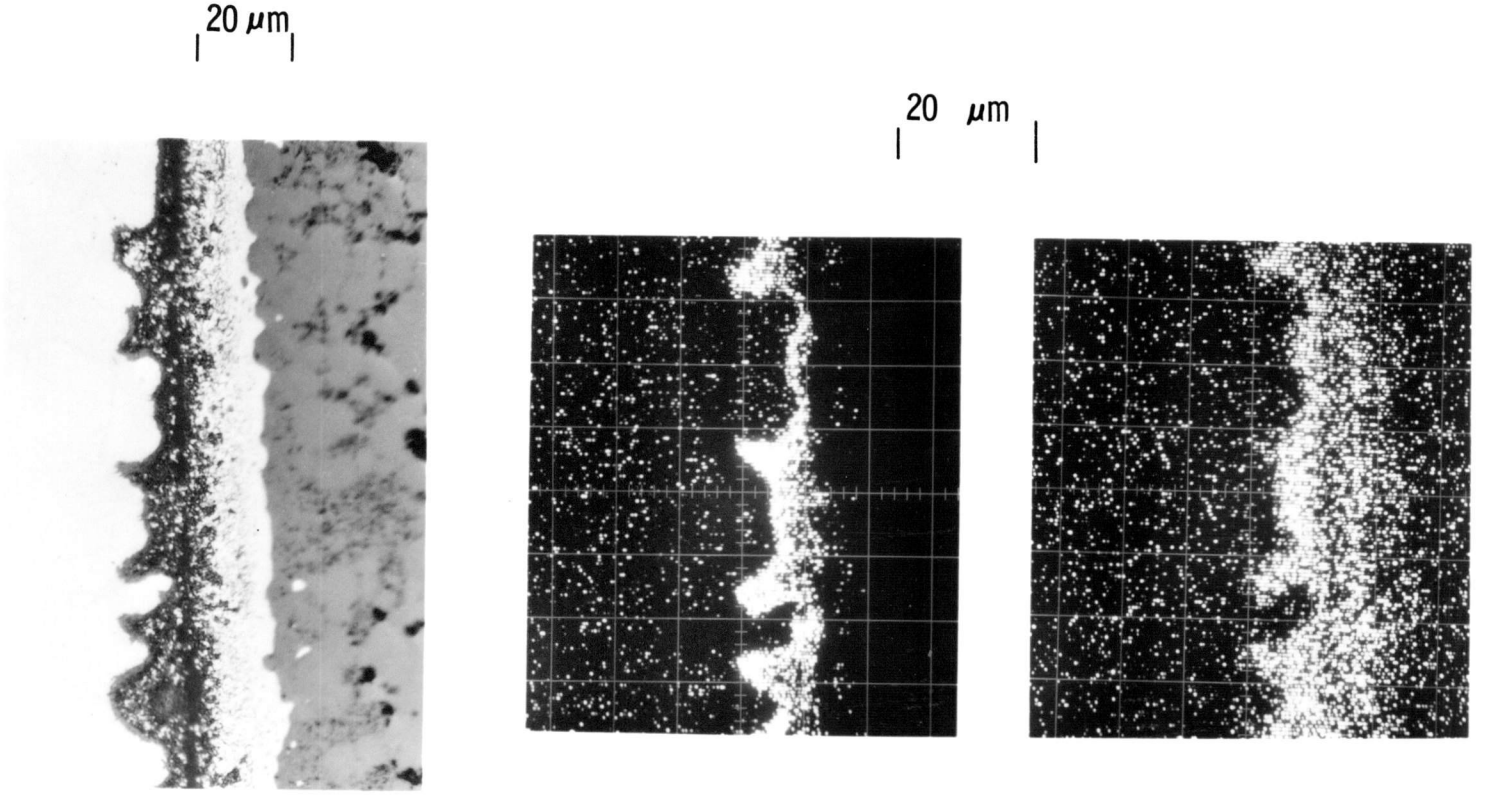

HEDL 7605-140.25

FIGURE 10

FCCI CHARACTERIZATION

- BURNUP TO 2.4 AT. %
  - $-< 680^{o}C$ MATRIX REACTION
  - $-> 680^{o}C$ INTERGRANULAR REACTION
- BURNUP 2.4 TO 5.3 AT. %
  - $-< 680^{o}C$ MATRIX REACTION
  - $-> 680^{o}C$ ADVANCED MATRIX
- IN CLADDING AHEAD OF REACTION FRONT
  - CARBIDES DISAPPEAR
  - CHROMIUM DEPLETED
  - NO FISSION PRODUCTS

HEDL 7605-140.10
FIGURE 11